Atmos. Chem. Phys. Discuss., 13, 10125–10156, 2013
www.atmos-chem-phys-discuss.net/13/10125/2013/
doi:10.5194/acpd-13-10125-2013

Atmospheric Chemistry and Physics Discussions
Open Access

Investigation of the "Elevated Heat Pump" hypothesis of the Asian monsoon using satellite observations

M. M. Wonsick, R. T. Pinker, and Y. Ma

Department of Atmospheric and Oceanic Science, University of Maryland, College Park, MD, USA

Received: 21 January 2013 – Accepted: 26 March 2013 – Published: 18 April 2013

Correspondence to: R. T. Pinker (pinker@atmos.umd.edu) and
M. M. Wonsick (mwonsick@atmos.umd.edu)

Published by Copernicus Publications on behalf of the European Geosciences Union.

Abstract

In recent years, the "Elevated Heat Pump" (EHP) hypothesis has been a topic of intensive research and controversy. It postulates that aerosol-induced anomalous mid- and upper-tropospheric warming above the Tibetan Plateau leads to an early onset and intensification of Asian monsoon rainfall. The finding is primarily based on results from a NASA Finite-Volume General Circulation Model run with and without radiative forcing from different types of aerosols. In particular, black carbon emissions from sources in Northern India and dust from Western China, Afghanistan, Pakistan, and Southwest Asia affected the modeled anomalous heating. Since the initial discussion of the EHP hypothesis in 2006, the aerosol-monsoon relationship has been addressed using various modeling and observational techniques. The current study takes an observational approach to detect signatures of the "Elevated Heat Pump" effect in the cloud cover and cloud type distributions as derived from Meteosat-5 observations over the Asian Monsoon region, supplemented with temperature data from the NCEP/NCAR Reanalysis and precipitation data from the Global Precipitation Climatology Project (GPCP). Cloud, convection, precipitation, and temperature features for the highest-aerosol years are compared with lower-aerosol content years during the period 2000–2005. Predicted precipitation features in China and Korea are found to be consistent with the hypothesis, but the early onset and intensification of monsoon rainfall over India are not observed. It is proposed that model inaccuracies and/or indirect aerosol effects caused the disagreement between observed and hypothesized behavior.

1 Introduction

Prediction of monsoon variability is of utmost importance for the safety and economic well-being of millions of people throughout India and other parts of Asia. Despite decades of research and improvement, climate models still fall short in accurately simulating and predicting the strength, timing and seasonal variability of the Asian mon-

ACPD
13, 10125–10156, 2013

soon. One reason for this situation is that unlike the rest of the tropics, Indian region monsoon modeling is highly sensitive to initial conditions (Sperber and Palmer, 1996; Krishnamurthy and Shukla, 2000; Cherchi and Navarra, 2003). Other particularly challenging aspects of the models are air–sea interactions, land surface effects, cloud and precipitation processes, and sea surface temperature feedbacks in the northern Indian Ocean (Li et al., 2001; Webster et al., 2002; Bollasina et al., 2008; Lucas-Picher et al., 2011).

As efforts continue to improve the performance of models by incorporating detailed processes and refined parameterizations, the role of aerosols in the monsoon system is gaining attention. Increased availability of aerosol data from in situ observations and remote sensing platforms makes this a promising area of exploration. Recent studies of aerosol effects on the Asian monsoon resulted in somewhat conflicting conclusions. One characteristic of aerosols is their tendency to cause shortwave radiation and temperature decrease at the earth's surface by reflecting incoming solar radiation – the so-called "solar dimming" effect (Stanhill and Cohen, 2001; Wild et al., 2004; Pinker et al., 2005). Another characteristic is the ability of aerosols such as dust and black carbon, which are abundant in the Asian monsoon region in springtime, to produce an atmospheric heating effect by absorbing solar radiation. Results from general circulation model (GCM) simulations have shown that solar dimming from aerosols can decrease the intensity of the Asian monsoon on multi-decadal time scales by weakening the land-sea temperature gradient in the region (Ramanathan et al., 2005; Chung and Ramanathan, 2006). Alternatively, aerosol-induced atmospheric heating has been linked to a strengthening of the monsoon in southern China, northern India, and the Bay of Bengal by impacting circulation patterns, vertical motions, and atmospheric stability (Menon et al., 2002; Lau et al., 2006). Meehl et al. (2008) have shown that the increased meridional temperature gradient due to heating from black carbon aerosols causes an increase in pre-monsoon rainfall (March through May) but a subsequent decrease in monsoon rainfall during June and July. The same behavior was reported by

ACPD
13, 10125–10156, 2013

Collier and Zhang (2009) based on runs of the NCAR CAM3 model with and without aerosols.

The focus of this study is to use observational data to examine the "Elevated Heat Pump" (EHP) hypothesis proposed by Lau et al. (2006). The basic premise of the hypothesis is that absorbing aerosols such as black carbon from northern India and dust from the deserts of western China, Afghanistan, Pakistan, and southwest Asia stack up against the foothills of the Himalayas in the pre-monsoon season and cause anomalous upper-tropospheric warming in the Tibetan Plateau region. The plausibility of aerosol transport is evident in Fig. 1, which shows the long-term mean of the general circulation near the surface in April. A relatively strong band of Westerlies extends from the deserts of southwest Asia toward the Indo-Gangetic Basin (IGB) at the base of the Himalayas. A southerly wind from northeast India contributes industrial black carbon to the aerosol loading in the IGB. The hypothesis proposes that warming by aerosol absorption causes the air to rise and act as an "Elevated Heat Pump", drawing in moist air from the Indian Ocean and causing an early onset of the Indian monsoon and intensification of monsoon rainfall. The sinking motion that completes the meridional circulation shifts northward, such that the southern part of the Indian subcontinent experiences dryer-than-normal conditions in the early part of the peak-monsoon season. Observational evidence of the EHP effect presented by Lau and Kim (2006) also indicates an early drawdown of the Indian monsoon season. Impacts on rainfall extend farther than the subcontinent itself, as the heat low established over the Tibetan Plateau is balanced by an elongated surface high pressure ridge oriented southwest to northeast from the northwestern Pacific through the northern South China Sea and southern Bay of Bengal into the central Indian Ocean. This pushes the typical *Mei-yu* rain belt northward and suppresses precipitation in the northern Indian Ocean, eastern China, and the western Pacific, while increasing rainfall totals in central India, the northern Arabian Sea, the northern Bay of Bengal, central China, and Korea. These conclusions were reached based on 10 yr runs of the NASA finite-volume GCM with and without aerosol forcing. The authors note that since these simulations neglected

ACPD
13, 10125–10156, 2013

important processes such as aerosol indirect effects, these findings must be considered suggestive, not conclusive.

The role of the Tibetan Plateau as an elevated heat source has long been recognized as one of the driving mechanisms of the Asian monsoon (Flohn, 1968; Yeh, 1981; Murakami, 1987; Ueda and Yasunari, 1998). Li and Yanai (1996) observed that the reversal of the meridional temperature gradient due to intense heating of the Tibetan Plateau in springtime coincides with the onset of the monsoon. The heating of the plateau prior to monsoon onset is mainly due to sensible heat flux in the semi-arid western part of the Plateau and latent heat flux in the more humid eastern region (Flohn, 1968; Yeh and Gao, 1979; Luo and Yanai, 1984; He et al., 1987). Taniguchi and Koike (2007) also showed that latent heat release from convective activity is responsible for heating through the depth of the troposphere in the eastern plateau, even before the rainy season begins. The EHP hypothesis suggests that warming caused by absorbing aerosols provides another mechanism to enhance the heating of the Tibetan Plateau. The potential impact of aerosol absorbing effects is magnified in this situation since the mass of the atmosphere above the plateau is roughly half of that near sea level and any heat added warms the air more effectively than over low-level terrain (Yeh, 1981). This can further strengthen the thermally induced circulation that draws in moisture from the Indian Ocean, bringing potential for increased convection.

Preliminary validation of the hypothesis was conducted by Lau and Kim (2006). Four high-aerosol years (1980, 1985, 1988, and 1991) and four low-aerosol years (1982, 1983, 1990, and 1992) were selected for the analysis based on the Total Ozone Mapping Spectrometer (TOMS) Aerosol Index (AI) (Hsu et al., 1999). The TOMS AI is a measure of how much the observed wavelength dependence of UV radiation backscattered from aerosols differs from that due to pure molecular scattering. The data record runs from 1978 through 2006, however data collected after mid-2000 are unreliable due to inhomogeneous degradation of the instrument's scanner mirror and therefore are not appropriate for trend analysis. Details of the problem can be found at: http://disc.sci.gsfc.nasa.gov/acdisc/TOMS.

ACPD
13, 10125–10156, 2013

Figure 2 shows the TOMS AI values for May of each year used in the analysis of Lau and Kim (2006). Of the high-aerosol years, 1988 and 1991 have significant levels of aerosols in the IGB with an AI of 3 or more. Of the low-aerosol years, 1982 and 1983 have AI values less than 2 in the IGB. The remaining 2 yr in each category are less extreme, with an average AI value between 2.25–2.50.

The evaluation was conducted using rainfall observations from the Global Precipitation Climatology Project (GPCP) (Huffman et al., 1997) and temperature and wind fields from the NCEP/DOE-R2 reanalysis data (Kanamitsu et al., 2002) composited separately for the high- and low-aerosol years. In agreement with the hypothesis, the following features were found in the high aerosol years: composite rainfall data showed an increase in precipitation in northern India in the early part of the season, spreading to all of India in June and July, and decreasing in August; enhanced ascent of warm air along the Himalayan foothills in May was evident in the composite wind fields; statistically significant correlation between high aerosol levels and warm upper tropospheric temperature anomalies in northern India and the Tibetan Plateau were found. Opposite behavior was observed during the low aerosol years.

Since the initial postulation of the EHP hypothesis, additional investigation on the topic has occurred (Wonsick et al., 2006; Guatam et al., 2009; Nigam and Bollasina, 2010). Bollasina et al. (2008) conducted an evaluation of the EHP hypothesis using regressions of various parameters such as precipitation, diabatic heating, winds, and radiative fluxes on the TOMS AI for May of the years 1979–1992. In contrast to the results of Lau and Kim (2006), they concluded that high aerosol loads in the IGB were associated with deficient precipitation throughout India in early spring. Additionally, their results suggest that land-surface processes set in motion by high aerosol concentrations, rather than the EHP mechanism, led to stronger monsoon rainfall during the months of June and July. Kuhlmann and Quass (2010) investigated the EHP effect using detailed, vertically resolved aerosol information from the Cloud-Aerosol Lidar and Infrared Pathfinder Satellite Observations (CALIPSO) data. They found the highest aerosol concentrations in the lower 5 km of the atmosphere with very little aerosol

ACPD
13, 10125–10156, 2013

reaching the altitude of the Tibetan Plateau. While peak shortwave heating in the lower troposphere closest to aerosol source regions reached the levels modeled in the Lau et al. (2006) study (0.2 K day^{-1}), elevated heating at the level of the Tibetan Plateau was only 0.05 K day^{-1}. Thus, they found no evidence of elevated heating that would be strong enough to influence large-scale monsoonal circulations.

To gain further insight on whether the EHP effect operates as proposed, this study utilizes newly available information on several crucial parameters for examining the existence of the EHP effect. In contrast to the previous studies that used TOMS AI, the springtime aerosol load in the IGB is determined from aerosol optical depth retrieved from the Multi-angle Imaging Spectroradiometer (MISR) (Bothwell et al., 2002). Retrieval of information on aerosols from TOMS is based on the backscattered radiance measurements in the range from 331 to 380 nm and provides a quantity known as the aerosol index (AI). Theoretical model simulations (Herman et al., 1997; Torres et al., 1998) have shown that the AI depends on aerosol optical depth (AOD), single scattering albedo, and aerosol height. It is a measure of how much the wavelength dependence of backscattered UV radiation from an atmosphere containing aerosols differs from that of a pure molecular atmosphere. Since the underlying Rayleigh scattering in the boundary layer is small, TOMS AI is more sensitive to aerosol loading at upper levels than near the surface. Retrieval of information on aerosols from the MISR instrument is based on the reflected radiation and provides information on the total columnar AOD.

Cloud extent and information on convection used in the analysis are based on a recently developed dataset derived from hourly Meteosat-5 satellite observations at 0.125° resolution (Wonsick et al., 2009). The high spatial resolution of this product allows a detailed investigation of cloud patterns in the Himalaya foothills region where much of the EHP effect is proposed to play out, and the high temporal resolution gives a good measure of the frequency of occurrence of convection. Finally, the monsoon behavior during individual years is analyzed in relation to the aerosol load in the IGB for each year. This approach is favored over analyzing the composite of several years

ACPD
13, 10125–10156, 2013

because the predicted patterns should be evident during extreme aerosol years if the EHP mechanism is operating as hypothesized.

The data used for the study will be described in Sect. 2. Sections 3 and 4 address methodology and results, respectively. A discussion of results is presented in Sect. 5, and conclusions are given in Sect. 6.

2 Data

2.1 Aerosols

The springtime aerosol loading is based on aerosol retrievals from MISR. The quality of the MISR AOD retrievals in the IGB was investigated by Prasad and Singh (2007). They compared AOD estimates from MISR and the Moderate Resolution Imaging Spectroradiometer (MODIS) (Kaufman et al., 1997; Tanre et al., 1997) to ground-based observations from the Aerosol Robotic Network (AERONET) for the years 2000–2005 and found that MISR retrievals were in closer agreement to ground observations than MODIS, attributable to the multi-angle viewing capabilities of the MISR instrument.

Figure 3 shows the MISR-based time series of mean AOD in the IGB for the years 2000–2005. The values are calculated by averaging the $1^\circ \times 1^\circ$ resolution monthly mean AOD data over the months of March–May for the domain in the IGB region. The years 2003 and 2004 had the highest springtime aerosol loading while aerosol content is much lower in the years 2001 and 2005.

2.2 Clouds and convection

Radiance observations from Meteosat-5 at hourly resolution are used to determine cloud amount and frequency of occurrence of convection. Total cloud amounts are derived using a 2-channel cloud detection scheme modified from the Clouds from AVHRR (CLAVR) algorithm used for the Advanced Very High Resolution Radiometer instrument aboard *NOAA* polar orbiting satellites (Stowe et al., 1999). The basic algorithm

ACPD
13, 10125–10156, 2013

compares 11.5 µm brightness temperature and visible reflectivity to empirically-derived cloud thresholds. The cloud detection is first performed at pixel-level (5 km) resolution and then re-projected onto a 0.125° latitude–longitude grid. Details of the algorithm and cloud analyses are given in Wonsick et al. (2009).

Convective cloud determination is based on Meteosat-5 11.5 µm brightness temperature and cloud optical depth as estimated by the University of Maryland Surface Radiation Budget (UMD/SRB) model (Pinker et al., 2003) driven with relevant observations from Meteosat-5. The cloud optical depth threshold for convective clouds is set to 23 as in the International Satellite Cloud Climatology Project (ISCCP) convective cloud algorithm (Rossow and Schiffer, 1991), and the brightness temperature cut-off is 250 K.

The cloud screening method is limited in its ability to accurately detect clouds at night when visible data are unavailable and the algorithm relies solely on the brightness temperature observations. For this reason, cloud data are only calculated where solar zenith angle (the angle between the sun and the pixel zenith) is less than 75°. For the domain of 51° E to 136° E longitude, this roughly corresponds to the hours of 00:00–13:00 UTC. The lack of nighttime cloud data does not appear to hamper the analysis for several reasons. Clouds and convection are analyzed in a relative sense of high-aerosol year versus low-aerosol year, so absolute values of cloud amount and convection have lesser importance. The percentage of convection missed overnight in the areas of interest is small because convection over land peaks in late afternoon in the Indian monsoon region (Gray and Jacobson, 1977; Dai, 2001; Islam et al., 2004). Frequency of convection patterns derived from Meteosat-5 show close agreement with rainfall amounts from GPCP, indicating that they capture the situation quite well. A comparison from June 2003 is shown in Fig. 4, and other months are similar.

2.3 Temperature and rainfall

As in the study by Lau and Kim (2006), temperature data from the NCEP/DOE-R2 reanalysis and precipitation data from GPCP are incorporated into the evaluation of the hypothesis.

ACPD
13, 10125–10156, 2013

3 Methodology

The years 2000–2005 are used in the study based on the overlap between availability of aerosol information from MISR and Meteosat-5 satellite imagery used to estimate cloud amount and convection. Based on the aerosol information shown in Fig. 3, the following classifications are made: 2003 and 2004 are high-aerosol years; 2001 and 2005 are low-aerosol years. The following verifiable aspects of the proposed EHP effect are assessed in relation to the aerosol load for each year: (1) the upper tropospheric temperature in the Tibetan Plateau region during April should be higher in the high aerosol years due to aerosol absorption of shortwave radiation, (2) convection and precipitation in the foothills of the Himalayas and in northern India should be higher in May during the high aerosol years due to the early onset of the monsoon, (3) convection and precipitation in southern India should be lower in June in the high aerosol years due to the northward shift in the subsiding branch of the meridional circulation over India, (4) convection and precipitation for the peak-monsoon season in the high aerosol years should be higher in northern India and the Bay of Bengal, and lower in eastern Asia, the northern Indian Ocean, and the western Pacific.

4 Results

4.1 Upper tropospheric temperature

According to the EHP hypothesis, in high-aerosol years the Tibetan Plateau should undergo anomalous upper tropospheric warming in April due to absorption of shortwave radiation by aerosols. Using TOMS AI and temperature observations from the Microwave Sounding Unit for the period 1979–2007, Gautam et al. (2009) reported a correlation between pre-monsoon aerosol loading in the IGB and increased middle- and upper-tropospheric temperature, most pronounced in May. This relationship was questioned by Nigam and Bollasina (2010), stating that the EHP hypothesis predicts

ACPD
13, 10125–10156, 2013

a 1-month lag between high aerosol loading and resultant tropospheric warming. Furthermore, in correlation analysis between TOMS AI and ERA-40 temperature data, they found statistically significant correlation only in the lower troposphere and only in regions farther south than what is predicted by the EHP.

For the average of the high aerosol years in our study, we show the latitude-height distribution of temperature anomaly in April over the latitude sector 70° E to 100° E from the NCEP/DOE-R2 Reanalysis (Fig. 5). The anomaly is based on climatology from 1968–1996. In agreement with the hypothesis, anomalous warming is observed directly above the Tibetan Plateau and on its slopes in the high-aerosol years. However, the distribution is not consistent with the distribution of temperature anomaly modeled in the study by Lau et al. (2006), which predicts even larger anomalies from 20–25° N corresponding to the highest concentrations of aerosol in the IGB being drawn northward and upward by the EHP effect. Instead, the observations show that the center of the anomaly is located north of 36° N and cannot be attributed to heating from the high aerosol load in the IGB.

4.2 Convection and precipitation

According to the EHP hypothesis, the anomalous warming observed over the Tibetan Plateau should accelerate the monsoon cycle and enhance convection in the foothills of the Himalayas in May during high-aerosol years. The difference between frequency of occurrence of convection in the foothills in May for the average of the high aerosol years (2003 and 2004) and the average of the low aerosol years (2001 and 2005) is shown in Fig. 6a. Frequency of occurrence of convection is computed for each point in the domain as the number of daytime hours in the month in which cloud top temperature and optical depth meet the convective cloud criteria outlined in Sect. 2.2. In the majority of the region there was actually less convection in the high aerosol years.

In addition to the proposed increase in convection in the foothills region, the simulations of Lau et al. (2006) predict enhanced precipitation in northern India (~ 20° N) during May of the high aerosol years. Figure 6b shows the difference in frequency of

ACPD
13, 10125–10156, 2013

occurrence of convection for all of India in May for the average of the high aerosol years (2003 and 2004) and the average of the low aerosol years (2001 and 2005). In contrast to what is expected, a significant increase in clouds and convection occurred during the high-aerosol years in southern India and the southern parts of the Arabian Sea and Bay of Bengal. The majority of the region north of 20° N experienced a decrease in convection during the high aerosol years.

Throughout the peak monsoon season (June–September) there are more discrepancies between the behavior predicted by the EHP hypothesis and the observed convection. By June, the subsiding branch of the meridional circulation that balances the forced ascent in the foothills should be well-established, causing a decrease in convection in southern India in the high-aerosol years. This aspect of the hypothesis is evident in Fig. 6c, which shows the difference in frequency of occurrence of convection between June for the average of the high aerosol years (2003 and 2004) and the average of the low aerosol years (2001 and 2005). The convection patterns in southern India are reversed from May, with less convection occurring in the high-aerosol years. Note however that this pattern holds throughout the majority of the sub-continent whereas the hypothesis prescribes that precipitation in the north in the high-aerosol years should still exceed that in the low-aerosol years because of the early progression of the monsoon.

Frequency of occurrence of convection for each July of 2000–2005 is displayed in Fig. 7. The year 2002, an extremely notable drought year, is the only year that had less convection on the Indian subcontinent than the high aerosol years (2003 and 2004). The year 2001 had the highest occurrence of convection, and 2005 had a considerable amount as well. This is contrary to the hypothesis, which predicts less precipitation in the low aerosol years.

As shown in Fig. 8, it is not until August that convection in northwest India and the northern Bay of Bengal in the high-aerosol years exceeds that in the low-aerosol years. This again contradicts the hypothesis, which asserts an early start to the monsoon and an early drawdown to the season.

ACPD
13, 10125–10156, 2013

Figure 9 shows the overall rainfall patterns for the combined months of June, July, and August for composites of the high (top) and low (bottom) aerosol years. Precipitation is derived from the GPCP database. There is less precipitation throughout most of India, the northern Bay of Bengal, and southern China during the high-aerosol year but more precipitation in the southern parts of the Arabian Sea and Bay of Bengal, central China, and Korea. These patterns disagree with what was predicted by the EHP hypothesis in the region of India and its surrounding waters, although they do agree over China and Korea.

5 Discussion

While it would have been of interest to perform the current analysis for the years used by Lau and Kim (2006), the sources of high-resolution cloud and aerosol information chosen for this study were not available until 1998 and 2000, respectively. Therefore, high and low aerosol years were selected from the period 2000–2005 based on the overlap between availability of aerosol information from MISR and the Meteosat-5 satellite imagery used to derive clouds and convection. While some of the behavior predicted by the EHP hypothesis was observed in this study, many events unfolded contrary to what was anticipated. Possible reasons why the observations did not agree with the predictions are explored here.

5.1 Model inaccuracies

Disparities in predicted monsoon behavior have been seen between fixed sea surface temperature (SST) models and coupled ocean-atmosphere models. The model used by Lau et al. (2006) to develop the EHP hypothesis used fixed SSTs and predicted enhanced Asian monsoon rainfall. Similarly, the study conducted by Menon et al. (2002) with a fixed SST model also found increased monsoon precipitation in parts of India and China and decreased precipitation in the northern Indian Ocean. Alternatively, sim-

ACPD
13, 10125–10156, 2013

ulations with coupled models by Ramanathan et al. (2005) and Meehl et al. (2008) resulted in less Asian monsoon precipitation. When the SSTs were allowed to respond to the decreased solar radiation in northern India and surrounding waters due to aerosol absorption, the meridional SST gradient weakened. Since this gradient is one of the major driving mechanisms of the monsoon, precipitation decreased in turn.

Although climate models are valuable tools for assessing the impact of changes in individual variables, the results can be skewed by model deficiencies and biases, as well as inaccuracies in initial conditions. Observation-based studies such as the current work are complementary to model simulations and can point to parts of the model that may need improvement. In this case, the observations support the model's prediction of upper tropospheric warming above the Tibetan Plateau but not the early onset, intensification, and early drawdown of the monsoon.

5.2 Cloud microphysics

Lau et al. (2006) acknowledge that the simulations leading to the EHP hypothesis address only direct aerosol effects (absorption and reflection of solar radiation), and that aerosol indirect and semi-direct effects could complicate matters. The indirect effects of aerosols can take several forms. In the first indirect effect (Twomey effect), aerosols act as cloud condensation nuclei to produce more numerous cloud droplets with smaller sizes. This implies higher cloud reflectance and cloud optical depths. The second indirect effect (also called the "cloud lifetime effect") directly follows: small cloud droplets are less efficient at generating precipitation, resulting in longer cloud lifetimes in polluted clouds than in cleaner clouds. Additionally, absorption of solar radiation by aerosols heats the atmosphere and may cause evaporation of clouds – the so-called semi-direct effect.

Evidence of this behavior of aerosols has been identified in the Asian monsoon region by numerous investigators. Heymsfield and McFarquhar (2001) analyzed aircraft data from flights made through polluted and clean clouds in the Indian Ocean during INDOEX (Ramanathan et al., 2001) and found a three-fold increase in droplet concentra-

ACPD
13, 10125–10156, 2013

tions and a 35 % decrease in droplet effective size in polluted clouds. Their simulations with a 1-D parcel model further implied a doubling of cloud optical depth with the high aerosol concentrations. Chylek et al. (2006) investigated the Twomey effect over the Indian subcontinent and surrounding waters using data from MODIS (Kaufman et al., 1997; Tanre et al., 1997). The cloud droplet effective radii retrieved from MODIS in clean months (the average of September months of the years 2000–2004) were up to 33 % larger than those retrieved in polluted months (Januarys of 2000–2004). Largest differences occurred in the land regions north of the Bay of Bengal, corresponding to regions of peak aerosol optical depth. Ackerman et al. (2000) found that the semi-direct effect from the haze layer observed during INDOEX 1998 and 1999 was responsible for a 25 % and 40 % decrease in fractional cloud cover, respectively.

Bollasina et al. (2008) observed that the semi-direct aerosol effect appeared to have a strong influence on pre-monsoon precipitation in the IGB. Their regression of rainfall on the TOMS aerosol index for the years 1979–1992 showed a link between high aerosol load and deficient springtime precipitation, which they attributed to dissipation of clouds through the aerosol semi-direct effect. To determine if such a link exists in the data used in the current study, the spatial correlation between MODIS AOD and Meteosat-5 derived frequency of occurrence of convection in the Himalaya foothills region in May is calculated for each year of the study period. Results are shown in Table 1. The negative correlation is apparent for all years, albeit more strongly for some years.

In explanation of the contrast between their findings and the enhancement of precipitation in the IGB in May observed by Lau and Kim (2006), Bollasina et al. (2008) noted the different mechanisms are at work in the eastern and western parts of the IGB. In the western region where the aerosol load is highest, precipitation appeared to be subdued by the aerosol semi-direct effect. Some increase in precipitation was seen in the eastern region, where the large-scale circulation flows northward over the Bay of Bengal, picking up abundant moisture and rising orographically when it encounters the Himalayas. Their results suggest that the high aerosol loading in the west may affect the

ACPD
13, 10125–10156, 2013

large-scale circulation in a manner that enhances this precipitation-producing mechanism in the east. However, the aerosol loading in the east is rather small and does not directly cause rising motion through the EHP mechanism. Furthermore, they assert that since Lau and Kim (2006) used a longitudinal average of precipitation across the IGB, the rainfall reduction in the west was masked by the activity in the east.

The details brought forth by the high-resolution Meteosat-5 data support the conclusions of Bollasina et al. (2008). Referring back to Fig. 6a, it is clear that the most significant increase in convection during the high-aerosol year occurs in the eastern regions. The western part of the IGB predominantly shows decreases in convection, or slight increases interspersed with decreases. Based on these results along with the negative correlation found between AOD and frequency of occurrence of convection, it appears that the aerosol semi-direct effect plays an important role in observed behavior of the monsoon for this period of study.

6 Conclusions

The high spatial and temporal resolution of Meteosat-5 satellite data along with improved aerosol information from sources such as MISR provide a unique opportunity to investigate processes that affect the Asian monsoon. This study exploits these capabilities to apply a different approach for evaluating the EHP hypothesis. It was found that in some aspects, observations were in agreement with the hypothesis but not in all of them. Specifically:

1. Anomalous warming over the Tibetan Plateau *was observed* but appears to be centered too far north to be associated with the absorbing aerosols in the IGB.

2. Enhanced convection in the foothills of the Himalayas and increased precipitation in northern India in May *was not observed*.

3. Suppression of precipitation in southern India in June *was observed*.

ACPD
13, 10125–10156, 2013

4. Early drawdown of monsoon *was not observed*.

5. Overall cloud and precipitation patterns for JJA

   (a) *did not match* hypothesis for India and surrounding oceans.

   (b) *did match* hypothesis for central China and Korea.

There are several factors that may have been responsible for discrepancies between the Meteosat-5 derived cloud and convection patterns and those predicted by the EHP hypothesis:

1. The impact of ocean/atmosphere coupling was not accounted for in the model simulation used to develop the EHP hypothesis.

2. The model simulation did not account for aerosol semi-direct effects, which seem to be responsible for reduced precipitation in the western portion of the IGB under high aerosol load.

We have isolated years of high and low aerosol loading using the most advanced methods of aerosol monitoring. It was found that the EHP effect was not detected in the years in which it should have been most observable. A study of longer duration would be useful to better determine the relative contributions of aerosol vs. larger-scale forcing. The satellite based information developed in this study and the improved aerosol information provide the needed information to analyze the patterns of clouds and convection in the IGB. The length of the data record from MISR is increasing and geostationary satellite coverage of the Asian monsoon region continues with the replacement of Meteosat-5 by Meteosat-7 in 2006. More detailed information on aerosol absorbing properties in the IGB for the year 2009 has become available from the observing campaigns coordinated through the Joint Aerosol-Monsoon Experiment (JAMEX) (Lau et al., 2008) and has been reported on by Guatam et al. (2011). In the present study we have developed a methodology to investigate aerosol-monsoon interactions with high-resolution cloud and convection observations from Meteosat-5. These upcoming

ACPD
13, 10125–10156, 2013

advancements in observations will set the stage to extend the present study to longer time periods that encompass a larger number of extreme aerosol years.

Acknowledgements. This work was supported under NASA grant NNG05GB35G to the University of Maryland and benefited from NASA grant NNX08AN40A from the Science Mission Directorate-Division of Earth Science. The authors wish to thank Yves Govaerts and the staff at the European Organisation for the Exploitation of Meteorological Satellites (EUMETSAT) Archive and Retrieval Facility for providing the Meteosat-5 observations and consulting on the calibration. Thanks are also due to the National Snow and Ice Data Center (NSIDC) at the University of Colorado, Boulder, CO, for providing the IMS snow data, the NASA/GSFC TOMS group for providing the TOMS aerosol data, and to NOAA/OAR/ESRL PSD, Boulder, Colorado, USA for providing the Reanalysis 2 data. MISR data were downloaded from the Goddard Earth Sciences Data and Information Services Center (GES DISC) Giovanni web site.

References

Ackerman, A. S., Toon, O. B., Stevens, D. E., Heymsfield, A. J., Ramanathan, V., and Welton, E. J.: Reduction of tropical cloudiness by soot, Science, 288, 1042–1047, 2000.

Bollasina, M., Nigam, S., and Lau, K.-M.: Absorbing aerosols and summer monsoon evolution over South Asia: an observational portrayal, J. Climate, 23, 3221–3239, 2008.

Bothwell, G. W., Hansen, E. G., Vargo, R. E., and Miller, K. C.: The Multi-angle Imaging SpectroRadiometer science data system, its products, tools and performance, IEEE T. Geosci. Remote, 40, 1467–1476, 2002.

Cherchi, A. and Navarra, A.: Reproducibility and predictability of Asian summer monsoon in the ECHAM4-GCM, Clim. Dynam., 20, 365–379, 2003.

Chung, C. E. and Ramanathan, V.: Weakening of North Indian SST gradient and the monsoon rainfall in India and the Sahel, J. Climate, 19, 2036–2045, 2006.

Chylek, P., Dubey, M. K., Lohmann, U., Ramanathan, V., Kaufman, Y. J., Lesins, G., Hudson, J., Altmann, G., and Olsen, S.: Aerosol indirect effect over the Indian Ocean, Geophys. Res. Lett., 33, L06086, doi:10.1029/2005GL025397, 2006.

Collier, J. C. and Zhang, G. J.: Aerosol direct forcing of the summer Indian monsoon as simulated by the NCAR CAM3, Clim. Dynam., 32, 313–332, doi:10.1007/s00382-008-464-9, 2009.

Dai, A.: Global precipitation and thunderstorm frequencies, Part 2: Diurnal variations, J. Climate, 14, 1112–1128, 2001.
Flohn, H.: Contributions to a meteorology of the Tibetan Highlands, in: Atmos. Sci. Paper No. 130, Colorado State University, Fort Collins, CO, 120 pp., 1968.
Gray, W. M. and Jacobson, R. W.: Diurnal variation of deep cumulus convection, Mon. Weather Rev., 105, 1171–1188, 1977.
Gautam, R., Hu, N. C., Lau, K.-M., Tay, S.-C., and Kafatos, M.: Enhanced pre-monsoon warming over the Himalayan–Gangetic region from 1979 to 2007, Geophys. Res. Lett., 36, L07704, doi:10.1029/2009GL037641, 2009.
Gautam, R., Hsu, N. C., Tsay, S. C., Lau, K. M., Holben, B., Bell, S., Smirnov, A., Li, C., Hansell, R., Ji, Q., Payra, S., Aryal, D., Kayastha, R., and Kim, K. M.: Accumulation of aerosols over the Indo-Gangetic plains and southern slopes of the Himalayas: distribution, properties and radiative effects during the 2009 pre-monsoon season, Atmos. Chem. Phys., 11, 12841–12863, doi:10.5194/acp-11-12841-2011, 2011.
He, H., McGinnis, J. W., Song, Z., and Yanai, M.: Onset of the Asian summer monsoon in 1979 and the effect of the Tibetan Plateau, Mon. Weather Rev., 115, 966–1995, 1987.
Herman, J. R., Bhartia, P. K., Torres, O., Hsu, C., Seftor, C., and Celarier, E.: Global distribution of uv-absorbing aerosols from Nimbus 7/TOMS data, J. Geophys. Res., 102, 16911–16922, 1997.
Heymsfield, A. J. and McFarquhar, G. M.: Microphysics of INDOEX clean and polluted cumulus clouds, J. Geophys. Res., 106, 28653–28673, 2001.
Hsu, N. C., Herman, J. R., Gleason, J. F., Torres, O., and Seftor, C. J.: Satellite detection of smoke aerosols over a snow/ice surface by TOMS, Geophys. Res. Lett., 26, 1165–1168, 1999.
Huffman, G., Adler, R. F., Arkin, P., Chang, A., Ferraro, R., Gruber, A., Janowiak, J., McNab, A., Rudolf, B., and Schneider, U.: The Global Precipitation Climatology Project (GPCP) combined precipitation dataset, B. Am. Meteorol. Soc., 78, 5–20, 1997.
Islam, M. N., Hayashi, T., Uyeda, H., Terao, T., and Kikuchi, K.: Diurnal variations of cloud activity in Bangladesh and north of the Bay of Bengal in 2000, Remote Sens. Environ., 90, 378–388, 2004.
Kanamitsu, M., Ebisuzaki, W., Woolen, J., Yang, S.-K., Hnilo, J. J., Fiorino, M., and Rotter, G. L.: NCEP/DOE AMIP-II reanalysis (R-2), B. Am. Meteorol. Soc., 83, 1631–1643, 2002.

ACPD
13, 10125–10156, 2013

Kaufman, Y., Tanré, D., Remer, L. A., Vermote, E. F., Chu, A., and Holben, B. N.: Operational remote sensing of tropospheric aerosols over land from EOS moderate resolution imaging spectroradiometer, J. Geophys. Res., 102, 17051–17067, 1997.
Krishnamurthy, V. and Shukla, J.: Intraseasonal and interannual variability of rainfall over India, J. Climate, 13, 4366–4377, 2000.
Kuhlmann, J. and Quaas, J.: How can aerosols affect the Asian summer monsoon? Assessment during three consecutive pre-monsoon seasons from CALIPSO satellite data, Atmos. Chem. Phys., 10, 4673–4688, doi:10.5194/acp-10-4673-2010, 2010.
Lau, K.-M. and Kim, K. M.: Observational relationships between aerosol and Asian monsoon rainfall, and circulation, Geophys. Res. Lett., 33, L21810, doi:10.1029/2006GL027546, 2006.
Lau, K.-M., Kim, M. K., and Kim, K. M.: Asian summer monsoon anomalies induced by aerosol direct forcing: the role of the Tibetan Plateau, Clim. Dynam., 26, 855–864, 2006.
Lau, K. -M., Ramanathan, V., Wu, G. -X., Li, Z., Tsay, S. C., Hsu, C., Sikka, R., Holben, B., Lu, D., Tartari, G., Chin, M., Koudelova, P., Chen, H., Ma, Y., Huang, J., Taniguchi, K., and Zhang, R.: The joint aerosol-monsoon experiment: a new challenge for monsoon climate research, B. Am. Meteorol. Soc., 89, 369–383, doi:10.1175/BAMS-89-3-369, 2008.
Li, C. and Yanai, M.: The onset and interannual variability of the Asian summer monsoon in relation to land–sea thermal contrast, J. Climate, 9, 358–375, 1996.
Li, T., Zhang, Y., Chang, C.-P., and Wang, B.: On the relationship between Indian Ocean sea surface temperature and Asian summer monsoon, Geophys. Res. Lett., 28, 2843–2846, doi:10.1029/2000GL011847, 2001.
Lucas-Picher, P., Christensen, J. H., Saeed, F., Kumar, P., Asharaf, S., Ahrens, B., Wiltshire, A. J., Jacob, D., and Hagemann, S.: Can regional climate models represent the Indian Monsoon? J. Hydrometeorol., 12, 849–868, doi:10.1175/2011JHM1327.1, 2011.
Luo, H. and Yanai, M.: The large-scale circulation and heat sources over the Tibetan Plateau and surrounding areas during the early summer of 1979, Part 2: Heat and moisture budgets, Mon. Weather Rev., 112, 966–989, 1984.
Meehl, G. A., Arblaster, J. M., and Collins, W. D.: Effects of black carbon aerosols on the Indian monsoon, J. Climate, 21, 2869–2882, 2008.
Menon, S., Hansen, J., Nazarenko, L., and Luo, Y. Climate effects of black carbon aerosols in China and India, Science, 297, 2250–2253, 2002.
Murakami, M.: Effects of the Tibetan Plateau, in: Monsoon Meteorology, edited by: Chang, C. P. and Krishnamurti, T. N., Oxford University Press, New York, 235–270, 1987.

ACPD
13, 10125–10156, 2013

Nigam, S. and Bollasina, M.: "Elevated heat pump" hypothesis for the aerosol-monsoon hydroclimate link: "grounded" in observations? J. Geophys. Res., 115, D16201, doi:10.1029/2009JD013800, 2010.

Pinker, R. T., Tarpley, J. D., and Laszlo, I.: Surface radiation budget in support of the GEWEX Continental-Scale International Project (GCIP) and the GEWEX American Prediction Project (GAPP), including the North American Land Data Assimilation System (NLDAS) Project, J. Geophys. Res., 108, 8844, doi:10.1029/2002JD003301, 2003.

Pinker, R. T., Zhang, B., and Dutton, E. G.: Do satellites detect trends in surface solar radiation? Science, 308, 850–854, 2005.

Prasad, A. K. and Singh, R. P.: Comparison of MISR-MODIS aerosol optical depth over the Indo-Gangetic basin during the winter and summer seasons (2000–2005), Remote Sens. Environ., 107, 109–119, 2007.

Ramanathan, V., Crutzen, P. J., Lelieveld, J., Mitra, A. P., Althausen, D., Anderson, J., Andreae, M. O., Cantrell, W., Cass, G. R., Chung, W. D., Clarke, A. D., Coakley, J. A., Collins, W. D., Conant, W. C., Dulac, F., Heintzenberg, J., Heymsfield, A. J., Holben, B., Howell, S., Hudson, J., Jayaraman, A., Kiehl, J. T., Krishnamurti, T. N., Lubin, D., McFarquhar, G., Novakov, T., Ogren, J. A., Podgorny, I. A., Prather, K., Priestley, K., Prospero, J. M., Quinn, P. K., Rajeev, K., Rasch, P., Rupert, S., Sadourny, R., Satheesh, S. K., Shaw, G. E., Sheridan, P., and Valero, F. P. J.: Indian Ocean Experiment: an integrated analysis of the climate forcing and effects of the great Indo-Asian haze, J. Geophys. Res., 106, 28371–28398, 2001.

Ramanathan, V., Chung, C., Kim, D., Bettge, T., Buha, L., Kiehl, J. T., Washington, W. M., Fu, Q., Sikka, D. R., and Wild, M.: Atmospheric brown clouds: impacts on South Asian climate and hydrological cycle, P. Natl. Acad. Sci. USA, 102, 5326–5333, doi:10.1073/pnas.0500656102, 2005.

Rossow, W. B. and Schiffer, R. A.: ISCCP cloud data products, B. Am.Meteorol. Soc., 71, 2–20, 1991.

Sperber, K. R. and Palmer, T. N.: Interannual tropical rainfall variability in general circulation model simulations associated with Atmospheric Model Intercomparison Project, J. Climate, 9, 2727–2750, 1996.

Stanhill, G. and Cohen, S.: Global dimming, a review of the evidence for a widespread and significant reduction in global radiation with a discussion of its probable causes and possible agricultural consequences, Agr. Meteorol., 107, 255–278, 2001.

ACPD
13, 10125–10156, 2013

Stowe, L. L., Davis, P. A., and McClain, E. P.: Scientific basis and initial evaluation of the CLAVR-1 global clear cloud classification algorithm for the Advanced Very High Resolution Radiometer, J. Atmos. Ocean. Tech., 16, 656–681, 1999.

Taniguchi, K. and Koike, T.: Increasing atmospheric temperature in the upper troposphere and cumulus convection over the eastern part of the Tibetan Plateau in the pre-monsoon season of 2004, J. Meteorol. Soc. Jpn., 85A, 271–294, 2007.

Tanre, D., Kaufman, Y., Herman, M., and Mattoo, S.: Remote sensing of aerosol properties over oceans using the MODIS/EOS spectral radiances, J. Geophys. Res., 102, 16971–16988, 1997.

Torres, O., Bhartia, P. K., Herman, J. R., Ahmad, Z., and Gleason, J.: Derivation of aerosol properties from satellite measurements of backscattered ultraviolet radiation: theoretical basis, J. Geophys. Res., 103, 17099–17110, 1998.

Ueda, H. and Yasunari, T.: Role of warming over the Tibetan Plateau in early onset of the summer monsoon over the Bay of Bengal and the South China Sea, J. Meteorol. Soc. Jpn, 76, 1–12, 1998.

Webster, P. J., Bradley, E. F., Fairall, C. W., Godfrey, J. S., Hacker, P., Houze, R. A., Jr., Lukas, R., Serra, Y., Hummon, J. M., Lawrence, T. D. M., Russell, C. A., Ryan, M. N., Sahami, K., and Zuidema, P.: The JASMINE pilot study, B. Am. Meteorol. Soc., 83, 1603–1630, doi:10.1175/BAMS-83-11-1603, 2002.

Wild, M., Ohmura, A., and Gilgen, H.: On the consistency of trends in radiation and temperature records and implications for the global hydrological cycle, Geophys. Res. Lett., 31, L11201, doi:10.1029/2003GL019188, 2004.

Wonsick, M. M., Pinker, R. T., and Liu, H.: Investigation of the “Elevated Heat Pump” effect on the Asian summer monsoon using cloud observations from Meteosat-5, AGU Fall Meeting, San Francisco, CA, 11–15 December 2006, A32C-05, 2006.

Wonsick, M. M., Pinker, R. T., and Govaerts, Y.: Cloud variability over the Indian monsoon region as observed from satellites, J. Appl. Meteorol. Clim., 48, 1803–1821, 2009.

Yeh, T.-C.: Some characteristics of the summer circulation over the Qinghai-Xizang (Tibet) Plateau and its neighborhood, B. Am. Meteorol. Soc., 62, 14–19, 1981.

Yeh, T. C. and Gao, Y. X.: The Meteorology of the Qinghai-Xizang (Tibet) Plateau, Science Press, Beijing, 278 pp., 1979.

ACPD
13, 10125–10156, 2013

Table 1. Spatial correlation between MODIS AOD and frequency of convection derived from Meteosat-5 for May of 2000–2005 for the region bounded by 25–33° N and 70–100° E (Himalaya foothills).

2000	2001	2002	2003	2004	2005
−0.58	−0.56	−0.67	−0.57	−0.57	−0.44

ACPD
13, 10125–10156, 2013

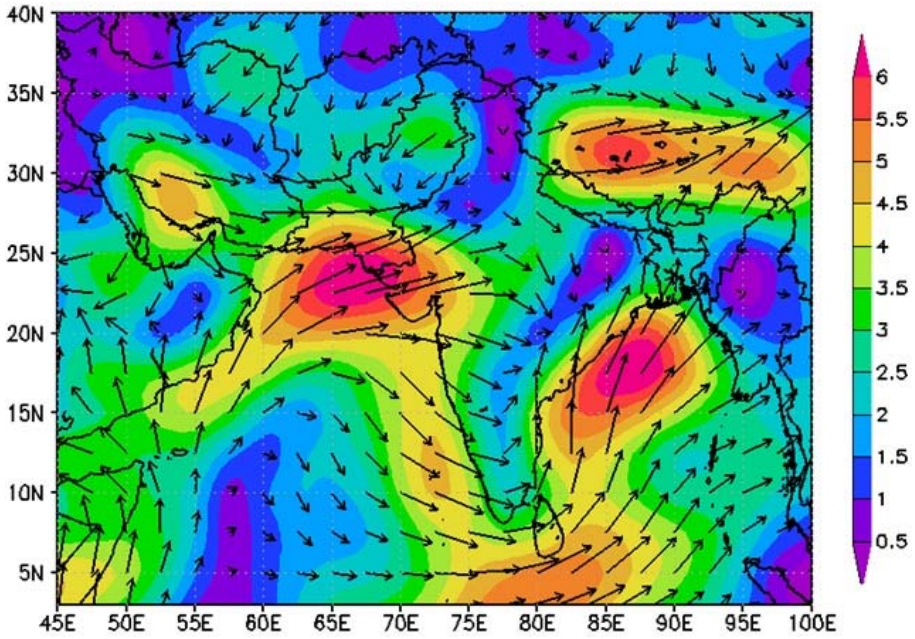

Fig. 1. Long term mean (1968–1996) 1000 mb wind vectors for April from NCEP/NCAR Reanalysis. Shading represents wind speed in $m\,s^{-1}$.

ACPD
13, 10125–10156, 2013

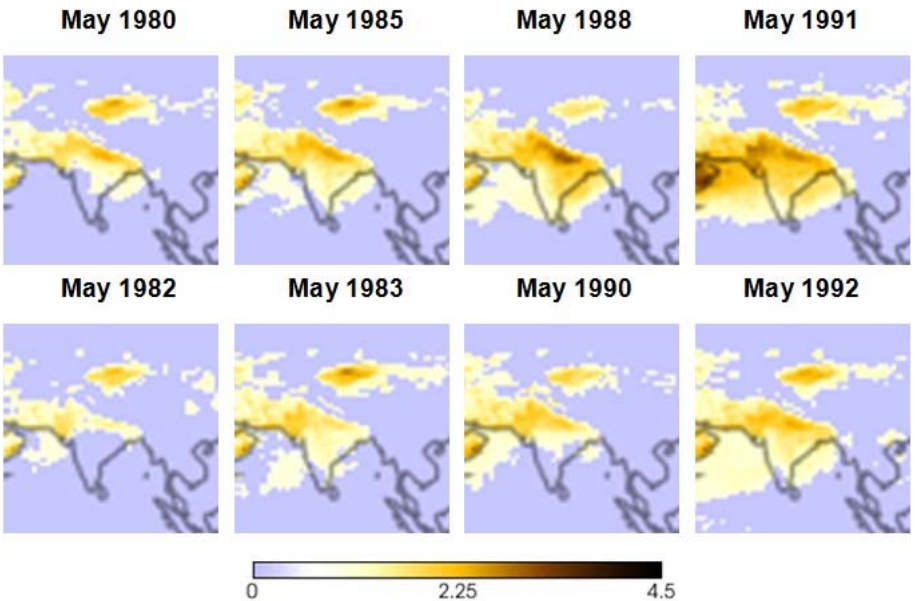

Fig. 2. TOMS aerosol index for May of the years used in the study by Lau et al. (2006). High aerosol years are shown in top row and low aerosol years are shown in bottom row.

ACPD
13, 10125–10156, 2013

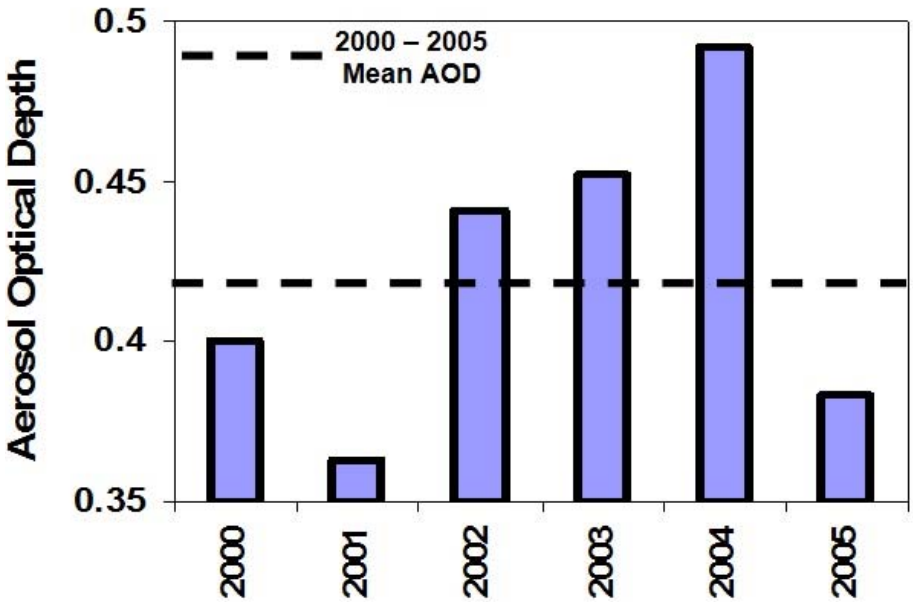

Fig. 3. Mean daytime aerosol optical depth at 0.55 µm in the Indo-Gangetic Basin (21–29.5° N, 73–90° E) averaged over the months of March–May, as derived from MISR.

ACPD
13, 10125–10156, 2013

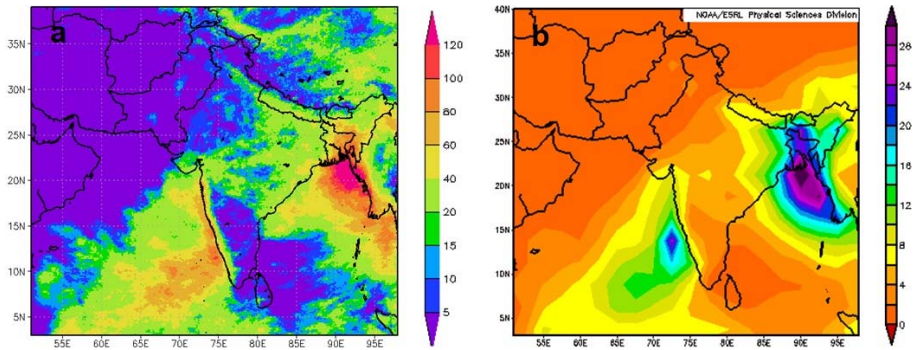

Fig. 4. (a) Frequency of occurrence of convection derived from Meteosat-5 and **(b)** monthly mean precipitation (mm day^{-1}) from GPCP for June 2003.

ACPD
13, 10125–10156, 2013

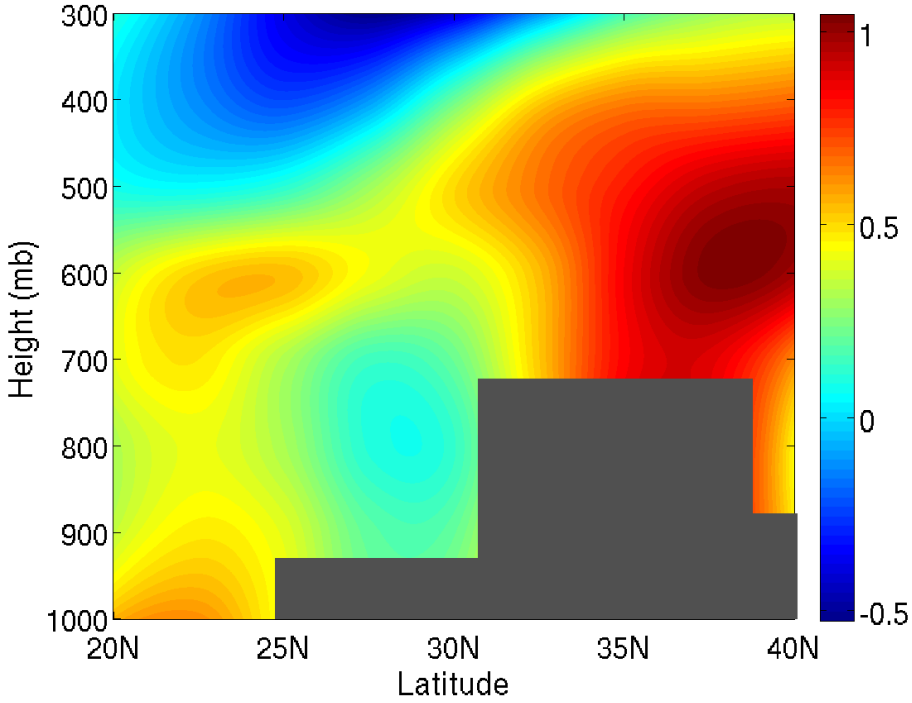

Fig. 5. Latitude-height distribution of temperature anomaly (°C) from NCEP/DOE-R2 Reanalysis over latitude sector 70 to 100° E for April of the average of high-aerosol years (2003 and 2004). Gray shaded area is an idealized representation of elevation of the Tibetan Plateau.

ACPD
13, 10125–10156, 2013

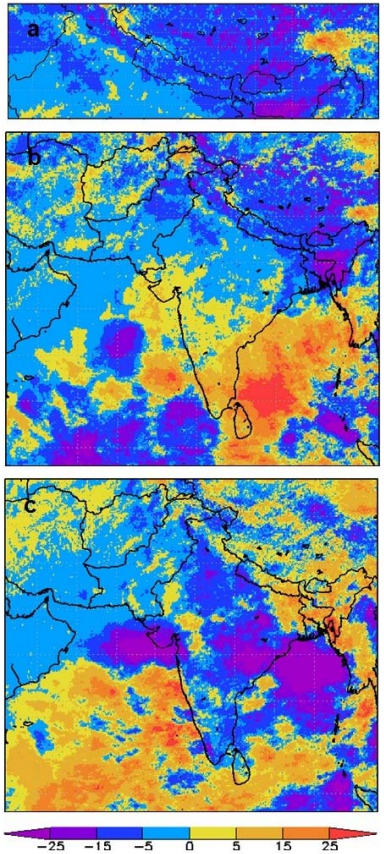

Fig. 6. Difference in frequency of occurrence of convection for the average of high aerosol years (2003 and 2004) minus the average of low aerosol years (2001 and 2005) for **(a)** detailed view of Himalaya foothills region in May, **(b)** India and surrounding waters in May, and **(c)** India and surrounding waters in June.

ACPD
13, 10125–10156, 2013

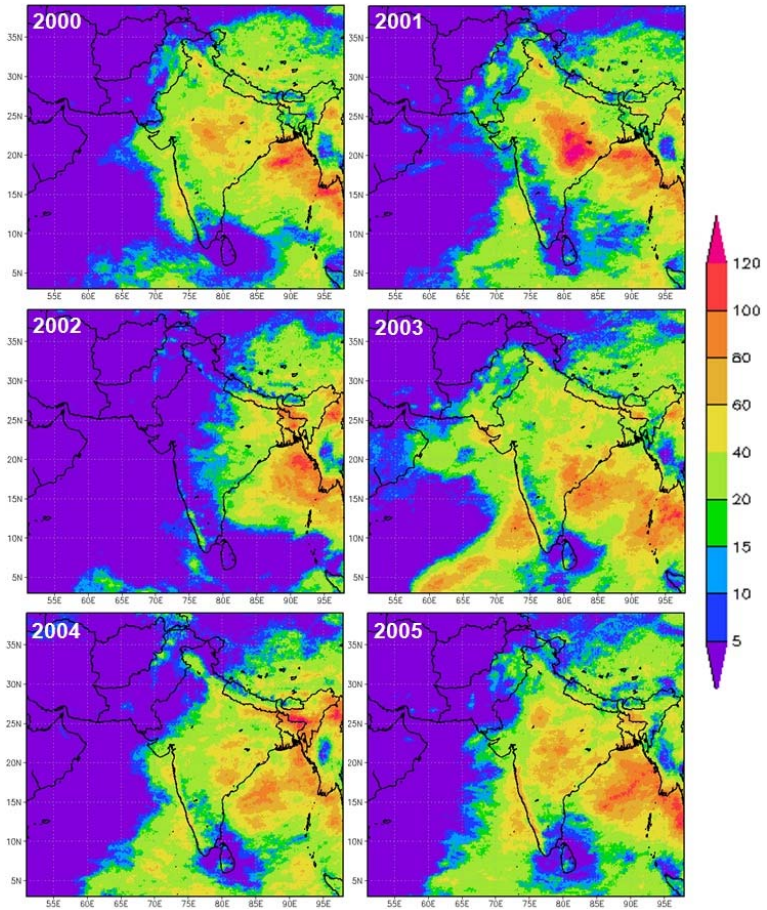

Fig. 7. Frequency of occurrence of convection for each July between 2000 and 2005.

ACPD
13, 10125–10156, 2013

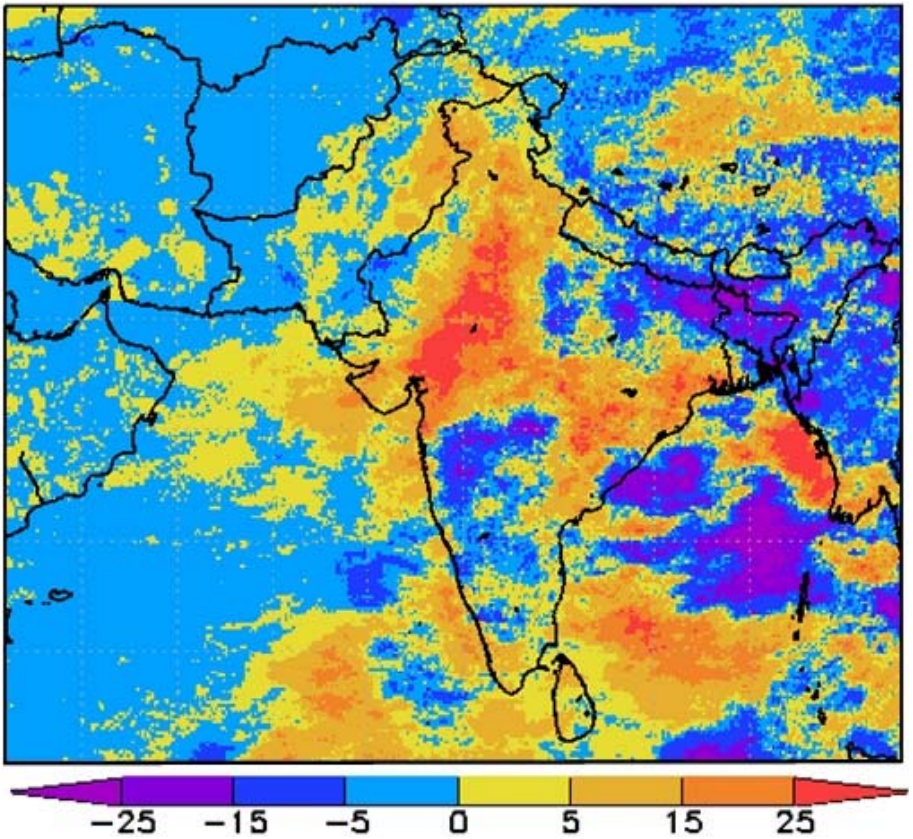

Fig. 8. Difference in frequency of occurrence of convection for India and surrounding waters during August for the average of high aerosol years (2003 and 2004) minus the average of low aerosol years (2001 and 2005).

ACPD
13, 10125–10156, 2013

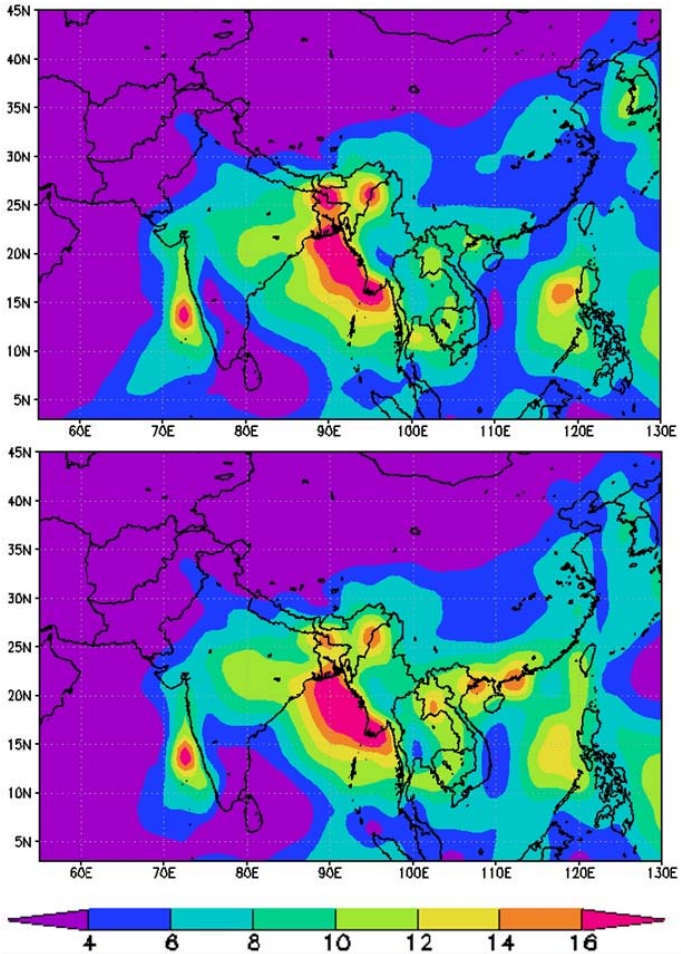

Fig. 9. GPCP rainfall (mm day^{-1}) for JJA for average of high aerosol years (top) and low aerosol years (bottom).

ACPD
13, 10125–10156, 2013